Rate Constants for $CF_3 + H_2 \rightarrow CF_3H + H$ and $CF_3H + H \rightarrow CF_3 + H_2$ Reactions in the Temperature Range 1100−1600 K

J. Hranisavljevic and J. V. Michael*

Chemistry Division, Argonne National Laboratory, Argonne, Illinois 60439

Received: June 1, 1998; In Final Form: June 29, 1998

The shock tube technique coupled with H-atom atomic resonance absorption spectrometry has been used to study the reactions (1) $CF_3 + H_2 \rightarrow CF_3H + H$ and (2) $CF_3H + H \rightarrow CF_3 + H_2$ over the temperature ranges 1168−1673 K and 1111−1550 K, respectively. The results can be represented by the Arrhenius expressions $k_1 = 2.56 \times 10^{-11} \exp(-8549K/T)$ and $k_2 = 6.13 \times 10^{-11} \exp(-7364K/T)$, both in cm^3 $molecule^{-1}$ s^{-1}. Equilibrium constants were calculated from the two Arrhenius expressions in the overlapping temperature range, and good agreement was obtained with the literature values. The rate constants for reaction 2 were converted into rate constants for reaction 1 using literature equilibrium constants. These data are indistinguishable from direct k_1 measurements, and an Arrhenius fit for the joint set is $k_1 = 1.88 \times 10^{-11} \exp(-8185K/T)$ cm^3 $molecule^{-1}$ s^{-1}. The $CF_3 + H_2 \rightarrow CF_3H + H$ reaction was further modeled using conventional transition-state theory, which included ab initio electronic structure determinations of reactants, transition state, and products.

Introduction

CF_3 abstraction reactions are of importance for establishing the combustion mechanism of the flame-inhibiting agent CF_3Br.[1−4]

$$CF_3 + H_2 \rightarrow CF_3H + H \quad (1)$$

Reaction 1 is considered to be one of the major routes for the formation of CF_3H in the CF_3Br-H_2 oxidation system.[2−4] Several relative kinetics studies of reaction 1 in the temperature range 296−1132 K have been carried out,[5−9] and a BEBO calculation of the Arrhenius parameters has also been reported.[10] However, no absolute kinetics measurements for this reaction are available to date. In this work, a direct shock tube kinetics study of reaction 1 is presented over the temperature range 1168−1673 K.

Rate constants for the reverse reaction,

$$CF_3H + H \rightarrow CF_3 + H_2 \quad (2)$$

have also been measured in the temperature range 1111−1550 K. By use of the two data sets for reactions 1 and 2, equilibrium constants have been calculated and compared to literature values[11] in the overlapping temperature range. In addition, conventional transition-state theoretical (CTST) calculations, which are based on an ab initio potential energy surface, have been applied to reaction 1 to predict the thermal rate behavior. These theoretical results help to make a connection between the present absolute high-temperature measurements and the low-temperature relative data[5−9] and to establish the kinetics behavior over the entire temperature range for reaction 1, 296−1673 K.

Experimental Section

The present experiments were performed with the shock tube (ST) technique, and the method and the apparatus currently being used have been previously described.[12,13] Therefore, only a brief description of the experiment will be presented here.

The apparatus consists of a 7-m (4-in. o.d.) 304 stainless steel tube separated from the He driver chamber by a 4-mil unscored 1100-H18 aluminum diaphragm. The tube was routinely pumped between experiments to less than 10^{-8} Torr by an Edwards Vacuum Products model CR100P packaged pumping system. The velocity of the shock wave was measured with eight equally spaced pressure transducers (PCB Piezotronics, Inc., model 113A21) mounted along the end portion of the shock tube, and temperature and density in the reflected shock wave regime were calculated from this velocity and include corrections for boundary layer perturbations.[14−16] The 4094C Nicolet digital oscilloscope was triggered by delayed pulses that derive from the last velocity gauge signal.

In the $CF_3 + H_2$ experiments, CF_3 radicals were produced by the thermal decomposition of either CF_3I or $(CF_3)_2CO$. Thermal decomposition of CF_3I has been well documented in previous work.[17] The lower limit of the examined temperature range was determined by the rate of CF_3I decomposition and the upper limit by the onset of the $I + H_2$ reaction. For CF_3 production from $(CF_3)_2CO$ at the lower temperature end, the limiting factor is incomplete $(CF_3)_2CO$ decomposition. However for this dissociation there are no kinetics data available to our knowledge. By analogy to $(CH_3)_2CO$,[18] the assumption was made that at 1325 K (the lowest temperature for CF_3 production from $(CF_3)_2CO$), the first-order rate constant for $(CF_3)_2CO$ thermal decomposition would be on the order of $\sim$1000 s^{-1}. To prevent this incomplete thermal decomposition from affecting the measured rate constants at lower temperatures, the data were analyzed by excluding the initial 500-μs portion. The limitation for measuring rate constants at the high-temperature end was the onset of direct H_2 thermal decomposition. In the $CF_3H + H$ experiments H atoms were produced from the thermal decomposition of C_2H_5I, as described previously.[19,20] The low-temperature measurements were limited by incomplete thermal

* Author to whom correspondence should be addressed, D-193, Bldg. 200. Phone: (630) 252-3171. Fax: (630) 252-4470. E-mail: Michael@anlchm.chm.anl.gov.

S1089-5639(98)02432-3 CCC: $15.00
Published on Web 09/09/1998

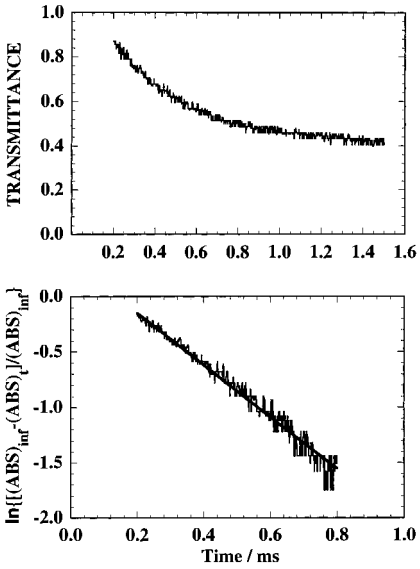

Figure 1. Top: transmittance decrease for $CF_3 + H_2 \rightarrow CF_3H + H$. Bottom: first-order buildup plot according to eq 3. $k^{1st} = 2304 \pm 128$ s^{-1} for an experiment at $P_1 = 15.83$ Torr and $M_s = 2.172$. $T_5 = 1191$ K, and $[H_2] = 1.324 \times 10^{17}$ cm^{-3}. The corresponding second-order rate constant is 1.740×10^{-14} cm^3 $molecule^{-1}$ s^{-1}.

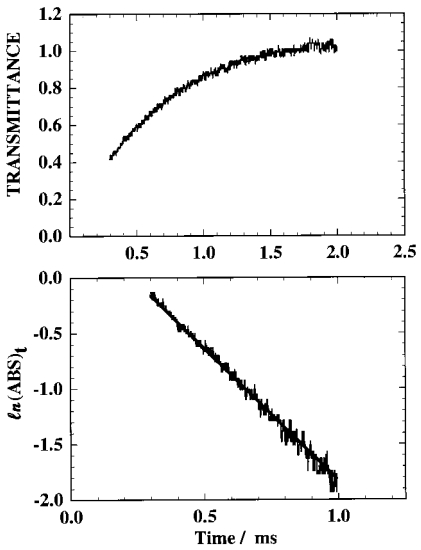

Figure 2. Top: transmittance increase for $CF_3H + H \rightarrow CF_3 + H_2$. Bottom: first-order decay plot according to eq 4. $k^{1st} = 2445 \pm 40$ s^{-1} for an experiment at $P_1 = 15.99$ Torr and $M_s = 2.234$. $T_5 = 1268$ K, and $[CF_3H] = 1.612 \times 10^{16}$ cm^{-3}. The corresponding second-order rate constant is 1.517×10^{-13} cm^3 $molecule^{-1}$ s^{-1}.

dissociation of C_2H_5I and, at higher temperatures, by the onset of CF_3H thermal decomposition.

In both $CF_3 + H_2$ and $CF_3H + H$ experiments, H-atom atomic resonance absorption spectrometric (ARAS) detection was used to follow $[H]_t$, as described previously.[21] The photometer system was radially located at a distance of 6 cm from the endplate. MgF_2 components were used in the photometer optics. The resonance lamp beam was detected by an EMR G14 solar blind photomultiplier tube. For the range of [H] used in these experiments, Beer's law is valid,[19,21] and therefore, $[H]_t = (ABS)_t/\sigma l$ where $(ABS)_t \equiv -\ln (I_t/I_0)$ (I_t and I_0 refer to time-dependent and incident photometric intensities, respectively, σ is the effective atomic cross section, and l is the absorption path length). Hence, only the relative absorbance changes need to be measured in both experiments, since $[H]_t$ is proportional to $(ABS)_t$.

For the $CF_3 + H_2$ experiment, the H-atom formation rate is not affected by secondary chemistry, and therefore, H-atom buildup constants follow the integrated rate law

$$\ln\left[\frac{(ABS)_\infty - (ABS)_t}{(ABS)_\infty}\right] = -k_1^{1st}t + \text{const} \qquad (3)$$

In the $CF_3H + H$ study, the H atoms are formed nearly instantaneously under the present conditions, and the H-atom decay constants follow the rate law

$$\ln (ABS)_t = -k_2^{1st}t + \text{const} \qquad (4)$$

The data were analyzed according to eqs 3 and 4 using linear least-squares methods. Typical results are shown in Figures 1 and 2. The derived values for k_{1st} and k for reactions 1 and 2 at each temperature are reported in Tables 1 and 2, respectively. Since $[H_2]$ and $[CF_3H]$ are effectively constant in the two experiments, the second-order rate constants are given by $k_1 = k_1^{1st}/[H_2]_0$, and $k_2 = k_2^{1st}/[CF_3H]_0$, and these are likewise listed in Tables 1 and 2.

Gases. Kr diluent for the experimental mixtures was obtained from Spectra Gases, Inc. (scientific grade, 99.997%), and was subjected to further purification by passage through a Gate Keeper inert gas purifier from Aeronex, Inc. He, used as

TABLE 1: Rate Data for the $CF_3 + H_2$ Reaction

P_1/Torr	M_s[a]	$\rho_5/(10^{18}$ $cm^{-3})$[b]	T_5/K[b]	k_1^{1st}/s^{-1}	k_1/cm^3 s^{-1} [c]
	$X_{(CF_3)_2CO} = 2.008 \times 10^{-7}$		$X_{H_2} = 2.050 \times 10^{-2}$		
15.97	2.385	2.929	1429	2720	4.531×10^{-14}
15.91	2.284	2.790	1325	1741	3.045×10^{-14}
15.91	2.411	2.960	1452	5375	8.859×10^{-14}
15.90	2.477	3.037	1523	6112	9.821×10^{-14}
15.87	2.325	2.836	1367	1982	3.410×10^{-14}
15.87	2.351	2.887	1394	3553	6.005×10^{-14}
15.84	2.504	3.056	1553	5673	9.055×10^{-14}
10.99	2.402	2.034	1449	3322	7.969×10^{-14}
10.96	2.529	2.145	1586	4800	1.092×10^{-13}
10.94	2.450	2.066	1501	4392	1.037×10^{-13}
10.92	2.604	2.198	1673	4582	1.017×10^{-13}
5.98	2.570	1.189	1633	2883	1.183×10^{-13}
5.97	2.516	1.162	1570	2971	1.248×10^{-13}
5.94	2.410	1.107	1453	1556	6.859×10^{-14}
5.93	2.524	1.158	1580	3140	1.323×10^{-13}
5.92	2.454	1.124	1501	2107	9.144×10^{-14}
	$X_{CF_3I} = 3.569 \times 10^{-7}$		$X_{H_2} = 2.804 \times 10^{-2}$		
15.98	2.232	2.753	1263	4109	5.324×10^{-14}
15.97	2.188	2.689	1220	1487	1.973×10^{-14}
15.93	2.229	2.740	1260	2909	3.787×10^{-14}
15.92	2.221	2.727	1252	2000	2.616×10^{-14}
15.92	2.200	2.689	1236	2740	3.635×10^{-14}
15.90	2.138	2.606	1172	708	9.696×10^{-15}
15.89	2.300	2.828	1331	4252	5.364×10^{-14}
10.96	2.288	1.937	1317	2577	4.746×10^{-14}
10.94	2.185	1.832	1213	1224	2.383×10^{-14}
10.93	2.194	1.832	1226	2169	4.223×10^{-14}
10.92	2.201	1.839	1234	1270	2.463×10^{-14}
10.91	2.116	1.749	1149	610	1.244×10^{-14}
	$X_{CF_3I} = 2.545 \times 10^{-7}$		$X_{H_2} = 4.953 \times 10^{-2}$		
15.96	2.159	2.667	1183	2216	1.678×10^{-14}
15.95	2.184	2.719	1199	2371	1.760×10^{-14}
15.92	2.147	2.651	1168	1594	1.214×10^{-14}
15.90	2.204	2.740	1218	3699	2.726×10^{-14}
15.83	2.172	2.673	1191	2304	1.740×10^{-14}

[a] The error in measuring the Mach number, M_s, is typically 0.5−1.0% at the 1 standard deviation level. [b] Quantities with the subscript 5 refer to the thermodynamic state of the gas in the reflected shock region. [c] The rate constants are derived as described in the text.

TABLE 2: Rate Data for the $CF_3H + H$ Reaction

P_1/Torr	M_s[a]	$\rho_5/(10^{18}$ cm$^{-3})$[b]	T_5/K[b]	k_2^{1st}/s^{-1}	k_2/cm^3 s^{-1} [c]
	$X_{C_2H_5I} = 1.594 \times 10^{-6}$		$X_{CF_3H} = 6.462 \times 10^{-3}$		
16.00	2.236	2.761	1269	3090	1.732×10^{-13}
15.88	2.406	2.790	1447	7141	3.961×10^{-13}
10.97	2.156	1.805	1187	1472	1.262×10^{-13}
10.94	2.241	1.893	1268	2274	1.859×10^{-13}
10.93	2.080	1.717	1114	1180	1.064×10^{-13}
10.92	2.077	1.712	1111	1026	9.270×10^{-14}
10.90	2.352	1.987	1386	4090	3.185×10^{-13}
10.88	2.185	1.820	1215	1724	1.466×10^{-13}
5.98	2.240	1.031	1270	1944	2.919×10^{-13}
5.98	2.195	1.006	1225	965	1.485×10^{-13}
5.93	2.324	1.067	1357	1789	2.595×10^{-13}
	$X_{C_2H_5I} = 5.848 \times 10^{-7}$		$X_{CF_3H} = 5.858 \times 10^{-3}$		
15.99	2.234	2.751	1268	2445	1.517×10^{-13}
15.98	2.088	2.547	1124	1002	6.715×10^{-14}
15.97	2.117	2.580	1155	1128	7.464×10^{-14}
15.88	2.239	2.740	1274	2912	1.817×10^{-13}
15.88	2.130	2.577	1172	2109	1.397×10^{-13}
10.93	2.148	1.793	1177	898	8.546×10^{-14}
10.96	2.214	1.867	1242	2395	2.190×10^{-13}
10.94	2.359	1.999	1396	3387	2.892×10^{-13}
10.90	2.361	1.993	1398	3479	2.980×10^{-13}
10.98	2.388	2.033	1427	3887	3.264×10^{-13}

[a] The error in measuring the Mach number, M_s, is typically 0.5−1.0% at the 1 standard deviation level. [b] Quantities with the subscript 5 refer to the thermodynamic state of the gas in the reflected shock region. [c] The rate constants are derived as described in the text.

received as the driver gas and also in the resonance lamp and atomic filter section, was ultrahigh purity grade (99.995%) and was obtained from Airco Industrial Gases. In the atomic filter section, H_2 from Airco Industrial Gases (prepurified, 99.995%) was used as received. $(CF_3)_2CO$, CF_3I, and CF_3H were all obtained from Aldrich Chemical Co. Inc. and were further purified by bulb-to-bulb distillation in a greaseless, all-glass, high-vacuum gas handling system. The middle third was retained. Mass spectral analyses showed that all samples were more than 99% pure.

Results

For reaction 1, initial curvature in the buildup plots results from incomplete decomposition, necessitating a long time analysis in order to obtain the first-order buildup constant. On the other hand, if H atoms are slowly formed from either $I + H_2$ or H_2 dissociation at higher temperatures, then curvature at long times results, necessitating an initial time analysis in buildup plots. In an effort to extend the temperature range, we carried out experiments at temperatures as low as 1085 K and as high as 1682 K, but these measurements had to be rejected due to these complications. Hence, bimolecular rate constants could only be unambiguously obtained over the limited temperature range 1168−1673 K. The results are given in Table 1 and are plotted in Arrhenius form in Figure 3 along with the linear least-squares line

$$k_1 = 2.56 \times 10^{-11} \exp(-8549K/T) \text{ cm}^3 \text{ molecule}^{-1} \text{ s}^{-1} \quad (5)$$

The individual data points in Figure 3 deviate from eq 5 by ±29% at the 1σ level.

For reaction 2, the measurements of bimolecular rate constants are summarized in Table 2 and Figure 4. Similar to the $CF_3 + H_2$ experiments, complications at the highest and lowest temperatures of the examined temperature range were avoided by analyzing the plots of ln $(ABS)_t$ against t in the initial or later stages, respectively. The rate constant measurements have

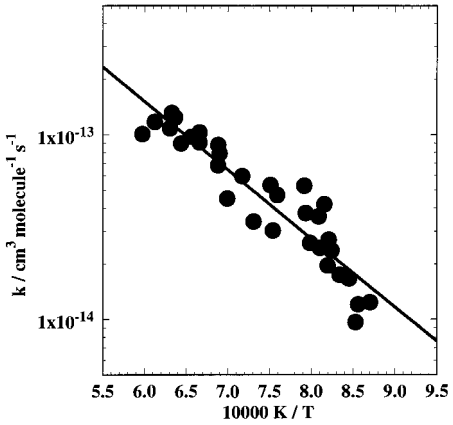

Figure 3. Arrhenius plot of the data from Table 1. The line is given by eq 5, and the solid circles are the individual data points.

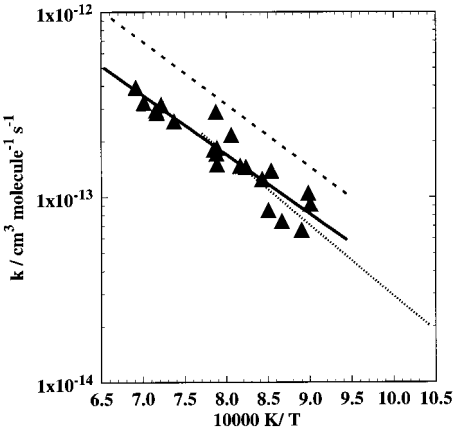

Figure 4. Arrhenius plot of the data from Table 2. The line is given by eq 6, and the solid triangles are the individual data points. The dashed line represents the rate constant expression reported by Takahashi and co-workers,[22] and the dotted line represents that reported by Richter et al.;[4] see eq 7.

also been represented by the Arrhenius equation giving the least-squares expression

$$k_2 = 6.13 \times 10^{-11} \exp(-7364K/T) \text{ cm}^3 \text{ molecule}^{-1} \text{ s}^{-1} \quad (6)$$

The data points shown in Figure 4 are within ±21% of the line calculated from eq 6 at the 1σ level.

Unlike reaction 1, there is one previous shock tube study on reaction 2 by Takahashi et al.[22] These workers also used H-atom ARAS (with H atoms generated from the dissociation of C_2H_5I) to measure the rate constants. Hence, the method is quite similar to this study. The main difference is that the present experiments were ∼20 times more sensitive in detecting $[H]_t$, thereby reducing the possibility of secondary reaction perturbations of decay constants. Even so, these results[22] are higher by only ∼30% than the measurements presented here and are therefore in good agreement within the error limits of the two data sets. Richter et al.[4] have also estimated k_2 in a flame study, reporting

$$k_2 = 1.93 \times 10^{-10} \exp(-8800K/T) \text{ cm}^3 \text{ molecule}^{-1} \text{ s}^{-1} \quad (7)$$

over the temperature range 960−1300 K. Both rate constant inferences[4,22] are shown along with the present data in Figure 4. As seen in the figure, the results summarized by eqs 6 and 7 are nearly superimposable.

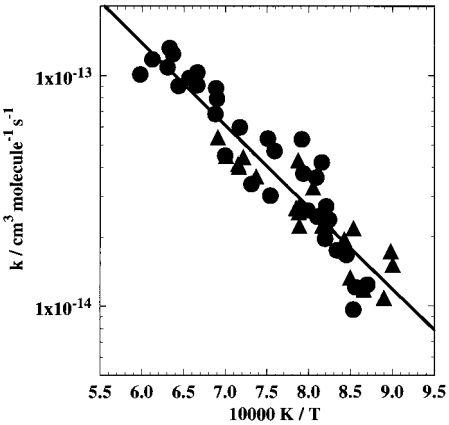

Figure 5. Composite Arrhenius plot for k_1 obtained by direct measurements (Table 1) and by the conversion of k_2 (Table 2) using equilibrium constants. The line is given by eq 8.

Discussion

Unlike the previous work on reaction 2,[22] the high sensitivity of the H-atom ARAS detection system used here completely eliminates the possibility of complications due to the onset of secondary reactions. This realization and the fact that both rate constants for reactions 1 and 2 were measured with exactly the same method, with the same apparatus, and in the same concentration range allows us to determine an apparatus-specific value for the equilibrium constants as $K_{eq} = k_1/k_2$. Hence, the two Arrhenius expressions, eqs 5 and 6, were used to evaluate the equilibrium constant at the midtemperature range of the two data sets, 1400 K. The K_{eq} value obtained was 0.18 ± 0.06 (i.e., $\pm 36\%$), in good agreement with the Janaf value of 0.128.[11] Hence, the data measured for $CF_3H + H$ were transformed into $CF_3 + H_2$ data using the K_{eq} values calculated from the Janaf tabulation. These transformed data are plotted in Figure 5 along with direct measurements for reaction 1. This composite set of data has then been least-squares fitted to an expression of the Arrhenius form as

$$k_1 = 1.88 \times 10^{-11} \exp(-8185K/T) \text{ cm}^3 \text{ molecule}^{-1} \text{ s}^{-1} \quad (8)$$

The individual data points deviate from the line by $\pm 28\%$ at the 1σ uncertainty level. From the plot in Figure 5, the data from the direct measurements and the data obtained by transformation through equilibrium constants are evenly scattered about the line calculated from eq 8. Hence, the present data suggest that the Janaf description is adequate within experimental error, implying $\Delta H^0_{01,2} = -1.564$ kcal mol^{-1} for the equilibrium process $CF_3 + H_2 \rightleftharpoons CF_3H + H$. To determine the error implied by the data, we additionally transformed the reaction 2 data under the assumption that $\Delta H^0_{01,2}$ ranged from 1 kcal mol^{-1} above to 1 kcal mol^{-1} below the Janaf value. Under both assumptions, the standard deviations of the combined sets then significantly increased from the linear least-squares Arrhenius representations. Values $\sim$0.6 kcal mol^{-1} above and below the Janaf $\Delta H^0_{01,2}$ could be tolerated and gave similar least-squares standard deviations. Hence, even though the present data are consistent with the Janaf endothermicity, they suggest that the value is only accurate to within ± 0.6 kcal mol^{-1}.

The experimental results for reaction 1, summarized by eq 8, can be compared to an evaluation given by Burgess et al.[23] who suggest

$$k_1 = (1.05 \times 10^{-22}) T^{3.0} \times \exp(-2667K/T) \text{ cm}^3 \text{ molecule}^{-1} \text{ s}^{-1} \quad (9)$$

Equation 9 predicts values only 11% higher and 30% lower than eq 8 over the present experimental temperature range. Since the goal of that work was to specify thermodynamic and kinetics information for modeling flame inhibition,[23] it is not necessary to modify k_1 from the value given. However, if eq 9 is used for temperatures lower than $\sim$1000 K, the values will undoubtedly be incorrect. Also, the values for the implied k_2 in that work will be slightly in error because they suggest $\Delta H^0_{01,2} = -2.9$ kcal mol^{-1}, in contrast to the present value of -1.564 kcal mol^{-1}.

In anticipation of theoretical rate constant calculations for reaction 1, we have additionally performed ab initio MP2/6-31G(d) level electronic structure calculations for both products and reactants. Similar electronic structure theory calculations have also been used earlier[3] for energy optimization and to find moments of inertia and vibration frequencies for the CF_3 and CF_3H molecules. The present calculations agree with this earlier work and imply $\Delta H^0_{01,2} = -2.4$ kcal mol^{-1} from the G2 heats of formation for CF_3[24] and CF_3H.[25] Since the Janaf endothermicity is $\Delta H^0_{01,2} = -1.564$ kcal mol^{-1}, the G2 estimate is within the ± 1 kcal mol^{-1} range usually claimed by the method.

By use of the Janaf endothermicity, harmonic values for K_{eq} were calculated for 1000$-$1700 K from the ab initio results. These values only differed from similarly calculated Janaf implied K_{eq} values by less than or equal to 1.2%, indicating that both frequencies and structures for CF_3 and CF_3H from the electronic structure calculations are essentially identical to the experimental values reported in the Janaf tables and listed in Table 3. This evaluation suggests that ab initio calculations for the transition state, carried out at the same level of theory, may also yield accurate values for both structure and frequencies. We therefore applied the same level of theory to determine structure, vibration frequencies, and energy for the transition state. The results, also listed in Table 3, were again nearly identical to those already presented by Berry et al.[3,26] except for the barrier height. Our calculations yield a zero-point energy-corrected barrier height for reaction 1 of 16.4, to be contrasted to 12.7 kcal mol^{-1} from Berry et al.

Berry et al.[3] have presented ab initio results and CTST rate constant calculations with tunneling corrections for the reactions $H + CH_nF_{4-n}$ ($0 \le n \le 4$), which includes calculations on reaction 2 and its reverse, reaction 1. Their results are presented without energy adjustments and are therefore truly ab initio. However, we have elected to carry out CTST calculations with Eckart tunneling, recognizing that the barrier height might have to be scaled if the present data are to be theoretically rationalized. Such adjustments are certainly warranted, since the G2 method for stable molecules is generally accurate to only $\sim \pm 1$ kcal mol^{-1} and the G2 method for transition states is accurate $\sim \pm 2-3$ kcal mol^{-1}.

The present unadjusted theoretical results (i.e., CTST with Eckart tunneling, the molecular parameters of Table 3, and $\Delta E^0_{01} = 16.4$ kcal mol^{-1}) are presented in Figure 6 as the dashed line. This prediction would suggest a 300 K value for k_1 of 1.03×10^{-21} cm^3 molecule^{-1} s^{-1}. As mentioned in the Introduction, there are several kinetics studies where the temperature dependence of rate constants for reaction 1 was measured relative to the rate constants for CF_3 self-recombination.[5-9] When the highest temperature results are neglected,[8] linear least-squares analysis of the composite data

TABLE 3: Molecular Parameters Used for Both Equilibrium and CTST/Eckart Theoretical Calculations

	CF_3	H_2	MP2 TS	CF_3H
energy in kcal mol^{-1}	0	0	16.4 (MP2) (14.058, adjusted)	−2.3 (G2), −1.564 (Janaf)
ν in cm^{-1}	500, 500, 701, 1090, 1259, 1259	4395	266, 266, 478, 647, 989, 1136, 1265, 1700, 1934*i*	508, 508, 700, 1137, 1152, 1152, 1376, 1376, 3035
moment of inertia product in g cm^2 $molecule^{-1}$	9.61×10^{-115}	4.60×10^{-41}	1.36×10^{-114}	9.72×10^{-115}

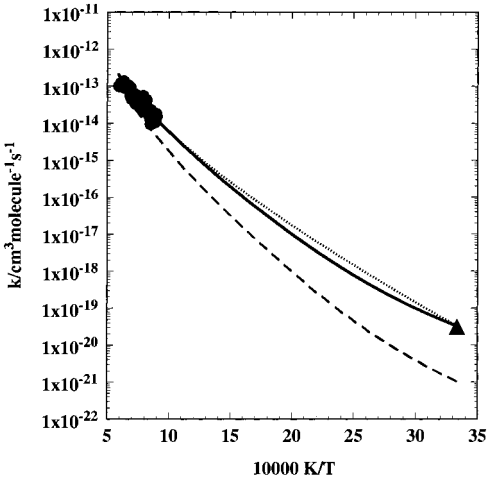

Figure 6. Comparison of the present experimental results (●) and k_1(300 K) derived in the text (▲) to theoretical and experimental results. The CTST/Eckart theoretical calculations are for barrier heights of 16.4 kcal mol^{-1} (- - -) and 14.058 kcal mol^{-1} (—). Equation 11 is the experimental three-parameter fit (···).

sets[5−7] (42 points between 295 and 604 K) gives the expression

$$k_1/k_r^{1/2} = (8.57 \pm 1.89) \times 10^{-7} \times \exp(-5351 \pm 92K/T)\ \mathrm{cm^{3/2}\ molecule^{-1/2}\ s^{-1/2}} \quad (10)$$

The 1σ error of the data points from eq 10 is ±31%. $k_1/k_r^{1/2}$ is 1.537×10^{-14} $cm^{3/2}$ $molecule^{-1/2}$ $s^{-1/2}$ at 300 K, and this, when combined with the predicted value from the unadjusted theoretical calculation, gives $k_r = 4.5 \times 10^{-15}$ cm^3 $molecule^{-1}$ s^{-1}. The reference reaction, $CF_3 + CF_3$ (+M) → C_2F_6 (+M), has been studied by several workers,[27−42] and a value as low as 4.5×10^{-15} cm^3 $molecule^{-1}$ s^{-1} has never been suggested. In fact, the room-temperature values span the range $(2.2-15) \times 10^{-12}$ cm^3 $molecule^{-1}$ s^{-1}. This indicates that the present ab initio barrier height estimate (16.4 kcal mol^{-1}) is too high and must be scaled in order to agree with experiment.

After review of the extensive database on the CF_3 recombination,[27−42] it is clear that there is no consensus agreement on the rate constant at room temperature. This is due in part to the use of quite different conditions of pressure and composition and the subsequent need to extrapolate results to the high-pressure limit. Hence, there have been at least three RRKM calculations performed on this system.[32,36,42] These calculations indicate that under most published experimental conditions of pressure, the recombination should be within 0.74−0.97 of the high-pressure limit at 300 K.[36,42] A simple average of eight room-temperature values gives k_r(300 K) = $(7.0 \pm 4.7) \times 10^{-12}$ cm^3 $molecule^{-1}$ s^{-1}; however, if two of the earlier determinations are eliminated,[28,31] the value becomes $(4.0 \pm 0.9) \times 10^{-12}$ cm^3 $molecule^{-1}$ s^{-1}. Allowing for some pressure falloff, we adopt as a reasonable value for $k_{r\infty}$, 4.5×10^{-12} cm^3 $molecule^{-1}$ s^{-1}.

k_1(300 K) can now be evaluated from the adopted value for $k_{r\infty}$ and eq 10, giving 3.26×10^{-20} cm^3 $molecule^{-1}$ s^{-1}. This room-temperature value is shown as the solid triangle in Figure 6. By use of the molecular parameters shown in Table 3, CTST/Eckart calculations can recover this value for k_1(300 K) if $\Delta E_{01}^0 = 14.058$ kcal mol^{-1}. The theoretical prediction of the temperature dependence is then shown as the solid line in Figure 6 and is reproduced to within ∼±25% by the three-parameter expression

$$k_1^{th} = (1.130 \times 10^{-29})T^{5.259} \times \exp(-2564K/T)\ \mathrm{cm^3\ molecule^{-1}\ s^{-1}} \quad (11)$$

over the temperature range 300−1700 K. Apparently theory can agree with both the 300 K and the present high-temperature experiments simply by adjusting the barrier height. We point out however that the theoretical values when combined with the relative expression, eq 10, imply k_r values of 4.5, 0.34, 0.26, and 0.35×10^{-12} cm^3 $molecule^{-1}$ s^{-1}, at the respective temperatures 300, 400, 500, and 600 K. On the other hand, we have nonlinear least-squares fitted the k_1 value at 300 K, 3.26×10^{-20} cm^3 $molecule^{-1}$ s^{-1} and the present high-temperature values summarized by eq 8, obtaining the expression

$$k_1^{exp} = (1.244 \times 10^{-24})T^{3.702} \times \exp(-3283K/T)\ \mathrm{cm^3\ molecule^{-1}\ s^{-1}} \quad (12)$$

to within ±3%. This equation is also plotted in Figure 6 as the dotted line. When eq 12 is combined with the relative rate expression, eq 10, respective k_r values at 300, 400, 500, and 600 K of 4.5, 1.2, 0.80, and 0.77×10^{-12} cm^3 $molecule^{-1}$ s^{-1} are obtained.

The question arises as to whether the theoretical, eq 11, or experimental, eq 12, representation is the better description. Of course, both descriptions strongly depend on the adequacy of k_r and k_1(300 K) derived from it; however, assuming that k_1(300 K) is correct, identification of the better description is still quite ambiguous for several reasons. Regarding theory, the extent of tunneling with the Eckart method may be overestimated and the use of CTST may be too simple. Even if these theoretical strategies are sufficient, the successful calculation still requires energy scaling. If any of the above assumptions are incorrect, then vibrational frequency adjustments in the transition state may additionally be required. Regarding the implied behavior for recombination, both descriptions suggest that $k_r(T)$ rapidly decreases with increasing temperature between 300 and 500 K; however, our theory would suggest that k_r then increases as temperature increases above 500 K. This disagrees with the only study where temperature was varied (k_r apparently increased from 11 to 25×10^{-12} cm^3 $molecule^{-1}$ s^{-1} between 297 and 457 K).[31] By contrast, a recent theoretical calculation, by Pesa et al.,[43] of high-pressure limits for the recombination using a derived potential energy surface along with flexible transition state-theory suggests decreasing values with increasing T $(13.42-6.15) \times 10^{-12}$ cm^3 $molecule^{-1}$ s^{-1} between 300 and 600 K). This new theoretical estimate reproduces neither the preferred value at room temperature nor the steepness of the decrease over the temperature range. Hence, we find that there is no firm way to decide which representation, eq 11 or 12, is best.

To conclude, even though the relative rate constant data summarized by eq 10 are really quite accurate and represented a significant experimental result when they were reported, we find that they still cannot be used to completely determine either k_1 or k_r. The present determination is really the first absolute determination for reaction 1, and it serves to define only the rate behavior at higher temperatures. No such absolute data exist at lower temperatures. Even though absolute data do exist for k_r, these data, undoubtedly for experimental reasons, are not sufficiently accurate to determine even the room-temperature rate constant. Clearly what is needed to complete the reactive description is further accurate and unambiguous experiments on either k_1 or k_r in the temperature range 300−600 K.

Acknowledgment. This work was supported by the U.S. Department of Energy, Office of Basic Energy Sciences, Division of Chemical Sciences, under Contract No. W-31-109-Eng-38. The authors thank Drs. S. S. Kumaran, M.-C. Su, and K. P. Lim for assistance in completing preliminary experiments. We also thank Dr. B. Ruscic for assistance with ab initio calculations and helpful discussions.

References and Notes

(1) Hidaka, Y.; Nakamura, T.; Kawano, H.; Koike, T. *Int. J. Chem. Kinet.* **1993**, *25*, 983.
(2) Westbrook, C. K. *Comb. Sci. Technol.* **1983**, *34*, 201.
(3) Berry, R. J.; Ehlers, C. J.; Burgess, D. R., Jr.; Zachariah, M. R.; Marshall, P. *Chem. Phys. Lett.* **1997**, *269*, 107.
(4) Richter, H.; Vandooren, J.; Van Tiggelen, P. J. *25th Symposium (International) on Combustion*; The Combustion Institute, Pittsburgh, PA, 1994; p 825.
(5) Kibby, C. L.; Weston, R. E., Jr. *J. Chem. Phys.* **1968**, *49*, 4825.
(6) Ayscough, P. B.; Polanyi, J. C. *Trans. Faraday Soc.* **1956**, *52*, 960.
(7) Fargash, M. B.; Moin, F. B.; Ocheret'ko, V. I. *Kinet. Katal.* **1968**, *9*, 762.
(8) Berces, T.; Marta, F.; Szilagyi, I. *J. Chem. Soc., Faraday Trans.* **1972**, *68*, 867.
(9) Pritchard, G. O.; Pritchard, H. O.; Schiff, H. I.; Trotman-Dickenson, A. F. *Trans. Faraday Soc.* **1956**, *52*, 849.
(10) Arthur, N. L.; Donchi, K. F.; McDonell, J. A. *J. Chem. Soc., Faraday Trans.* **1975**, *71*, 2431.
(11) Chase, M. W., Jr.; Davies, C. A.; Downey, J. R., Jr.; Frurip, D. J.; McDonald, R. A.; Syverud, A. N. *J. Phys. Chem. Ref. Data* **1985**, *14* (Suppl. 1).
(12) Michael, J. V. *Prog. Energy Combust. Sci.* **1992**, *18*, 327.
(13) Michael, J. V. In *Advances in Chemical Kinetics and Dynamics*; Barker, J. R., Ed.; JAI Press: Greenwich, 1992; Vol. I, pp 47−112, for original references.
(14) Michael, J. V.; Sutherland, J. W. *Int. J. Chem. Kinet.* **1986**, *18*, 409.
(15) Michael, J. V. *J. Chem. Phys.* **1989**, *90*, 189.
(16) Michael, J. V.; Fisher, J. R. *Proceedings of the 17th International Symposium on Shock Waves and Shock Tubes*; Kim, Y. W., Ed.; American Institute of Physics: New York, 1990; pp 210−215.
(17) Kumaran, S. S.; Su, M.-C.; Lim, K. P.; Michael, J. V. *Chem. Phys. Lett.* **1995**, *243*, 59.
(18) Ernst, J.; Spindler, K.; Wagner, H. Gg. *Ber. Bunsen-Ges. Phys. Chem.* **1976**, *80*, 645.
(19) Kumaran, S. S.; Su, M.-C.; Lim, K. P.; Michael, J. V. *26th Symposium (International) on Combustion*; The Combustion Institute, Pittsburgh, PA, 1996; p 605.
(20) Herzler, J.; Frank, P. *Ber. Bunsen-Ges. Phys. Chem.* **1992**, *96*, 1333.
(21) Lim, K. P.; Michael, J. V. *25th Symposium (International) on Combustion*; The Combustion Institute, Pittsburgh, PA, 1994; p 713 and references therein.
(22) Takahashi, K.; Inomata, T.; Abe, T.; Fukaya, H. *Proceedings of the 21st International Symposium on Shock Waves*; Houwing, A. F. P., Ed.; Panther Publishing: Fyshwick, Australia, 1997; p 163.
(23) Burgess, D. R., Jr.; Zachariah, M. R.; Tsang, W.; Westmoreland, P. R. *Prog. Energy Combust. Sci.* **1995**, *21*, 453.
(24) Ruscic, B. Unpublished G2 result, $\Delta H^0_{f0,CF_3} = -114.1$ kcal mol^{-1}.
(25) Curtiss, L. A.; Raghavachari, K.; Redfern, P.; Pople, J. A. *J. Chem. Phys.* **1997**, *106*, 1063.
(26) Marshall, P. Private communication, 1998.
(27) Ayscough, P. B. *J. Chem. Phys.* **1956**, *24*, 944.
(28) Ogawa, T.; Carlson, G. A.; Pimentel, G. C. *J. Phys. Chem.* **1970**, *74*, 2090.
(29) Basco, N.; Hathorn, F. G. M. *Chem. Phys. Lett.* **1971**, *8*, 291.
(30) Hiatt, R.; Benson, S. W. *Int. J. Chem. Kinet.* **1972**, *4*, 479.
(31) Skorobogatov, G. A.; Seleznev, V. G.; Slesar, O. N. *Dokl. Phys. Chem.* **1976**, *231*, 1292.
(32) Rossi, M.; Golden, D. M. *Int. J. Chem. Kinet.* **1979**, *11*, 775.
(33) Glanzer, K.; Maier, M.; Troe, J. *J. Phys. Chem.* **1980**, *84*, 1681.
(34) Velichko, A. M.; Gordon, E. B.; Nedelkin, A. A.; Nikitin, A. I.; Tal'roze, V. L. *High Energy Chem.* **1985**, *19*, 58.
(35) Plumb, I. C.; Ryan, K. R. *Plasma Chem. Plasma Process* **1986**, *6*, 205.
(36) Selamoglu, N.; Rossi, M. J.; Golden, D. M. *Chem. Phys. Lett.* **1986**, *124*, 68.
(37) Brown, C. E.; Orlando, J. J.; Reid, J.; Smith, D. R. *Chem. Phys. Lett.* **1987**, *142*, 213.
(38) Skorobogatov, G. A.; Dymov, B. P.; Lebedev, V. N.; Khripun, V. K. *Kinet. Katal.* **1987**, *28*, 682.
(39) Robertson, R. M.; Golden, D. M.; Rossi, M. J. *J. Phys. Chem.* **1988**, *92*, 5338.
(40) Skorobogatov, G. A.; Slesar, O. N.; Torbin, N. D. *Vestn. Leningr. Univ. Ser., Fiz. Khim.* **1988**, *4*, 30.
(41) Hidaka, Y.; Nakamura, T.; Kawano, H. *Chem. Phys. Lett.* **1989**, *154*, 573.
(42) Vakhtin, A. B. *Int. J. Chem. Kinet.* **1996**, *28*, 443.
(43) Pesa, M.; Pilling, M. J.; Robertson, S. H.; Wardlaw, D. M. *J. Phys. Chem.*, in press.